15 August 1999

ELSEVIER

Optics Communications 167 (1999) 15–22

OPTICS COMMUNICATIONS

www.elsevier.com/locate/optcom

Far-field diffraction of pulsed optical beams in dispersive media

Govind P. Agrawal

The Institute of Optics and Rochester Theory Center, University of Rochester, Rochester, NY 14627, USA

Received 29 January 1999; received in revised form 19 April 1999; accepted 9 June 1999

Abstract

Propagation of a pulsed optical beam (a train of ultrashort optical pulses) inside a linear dispersive medium is studied in the far field without making the paraxial approximation. This approach permits us to obtain analytical results that are valid for relatively large diffraction angles. Pulse characteristics are found to be affected considerably by the combination of diffraction and dispersion. In a weakly dispersive medium, pulses wider than a few optical cycles maintain their shape but experience temporal and spectral shifts whose magnitude depends on the diffraction angle. When the effects of group-velocity dispersion are included, the pulse width depends not only on the diffraction angle but also on the nature of dispersion (normal versus anomalous). Much larger off-axis pulse widths are predicted in the case of anomalous dispersion.

1. Introduction

With the advent of solid-state lasers capable of emitting a train of ultrashort optical pulses [1], considerable attention has focused on studying how such pulses are affected as they propagate inside a linear *nondispersive* medium [2–9]. Most studies assume a Gaussian spatial profile for the optical beam and a Gaussian temporal profile for the pulse shape. Kaplan has considered pulses of arbitrary shape [8] but focused mostly on the temporal evolution of the on-axis intensity. It was shown recently that a pulsed Gaussian beam does not remain Gaussian on propagation even in a linear nondispersive medium (such as free space) when pulses contain only a few optical cycles [9]. Moreover, the shape of the diffracted beam depends on temporal phase modulation or frequency chirp imposed on the pulse.

An interesting question that one may ask is how pulsed optical beams are affected when they propagate and diffract in a linear dispersive medium. Of course, dispersive broadening of optical pulses is a well-studied topic belonging to text books and has attracted renewed attention [10] with the advent of femtosecond-pulse lasers. However, most such studies decouple the diffraction and dispersion problem by assuming that the spatial profile of the beam does not change during propagation or assuming that the pulsed beam is propagating in a waveguide such as an optical fiber [11]. Even when diffraction and dispersion are considered simultaneously, it is common to employ the slowly varying envelope approximation, the use of which limits the analysis to pulses much broader than an optical cycle. However, considerable progress has been made over the last two years. Melamed and Felsen used an asymptotic technique to study pulsed-beam propagation in the paraxial far-field region without making the slowly varying envelope approximation [12]. Oughstun used the angular-spectrum approach and analyzed the pulsed-

0030-4018/99/$ - see front matter
PII: S0030-4018(99)00303-X

beam problem in a mathematically rigorous way considering both dispersion and attenuation [13]. Solhaug et al. used a similar approach to study edge-diffraction of a delta-function pulse by employing the Lorentz model for the dispersive medium [14].

In this paper, propagation of pulsed optical beams in a linear dispersive medium is studied approximately without using a specific model for the dispersive medium. Since the slowly varying envelope approximation is not made, the analysis is applicable to pulses shorter than a single cycle and, in principle, can be used to study propagation of terahertz radiation [15–17]. However, this paper focuses on optical pulses wider than a few optical cycles. This feature allows us to make several assumptions that simplify the analysis considerably. First, the pulse spectrum is assumed to be far from any medium resonances, and signal attenuation (that is necessarily frequency dependent in a causal dispersive dielectric [13]) is ignored. Second, we make use of the far-field approximation but avoid the paraxial approximation to ensure that the results are valid for large far-field angles. The general formalism is developed in Section 2 and applied to Gaussian beams containing pulses of arbitrary shape. Section 3 is devoted to study the case of weakly dispersive medium for which an analytical expression for the diffracted field can be obtained for arbitrary pulse shapes. The results show that diffraction leads to temporal and spectral shifts whose magnitudes vanishes only on axis and can be quite large even for relatively small diffraction angles. The effects of group-velocity dispersion (GVD) are studied in Section 4 where we show that the dispersive broadening of ultrashort pulses depends on the diffraction angle as well as on the nature of GVD (normal versus anomalous). The analysis predicts much larger off-axis pulse widths in the case of anomalous GVD.

2. Diffracted field

The pulsed-beam propagation problem is quite simple conceptually when the dispersive medium is linear since one can consider each Fourier component independently. Indeed, in a linear dispersive dielectric medium, Maxwell's equations for the electromagnetic field $E(\mathbf{r},t)$ can be solved in the frequency domain using the Helmholtz equation [18]

$$(\nabla^2 + \beta^2)\tilde{E}(\mathbf{r},\omega) = 0, \tag{1}$$

where $\tilde{E}$ is the Fourier component of E at the frequency ω and the propagation constant β obeys the dispersion relation

$$\beta(\omega) = n(\omega)\,\omega/c. \tag{2}$$

Here $n(\omega)$ is the frequency-dependent refractive index of the dispersive medium and c is the speed of light in vacuum. We assume that the medium is lossless and take $n(\omega)$ to be real. Inclusion of loss is straightforward and does not affect the results reported here qualitatively when the absorption is nearly frequency independent over the pulse spectrum. The vector nature of electromagnetic field is ignored assuming that the plane of polarization does not change during propagation.

We consider the case in which $\tilde{E}(\mathbf{r},\omega)$ is known at the plane $z = 0$ and Eq. (1) is solved in the region $z > 0$. By using the angular spectrum representation [18], the diffracted field can be obtained at each frequency ω. Taking the inverse Fourier transform, one can express the diffracted field formally in the form of a triple integral:

$$E(\mathbf{r},t) = \frac{1}{2\pi}\int\int\int A(p,q,\omega) \times \exp[i\beta(px+qy+mz) - i\omega t] \times dp\,dq\,d\omega, \tag{3}$$

where the angular spectrum $A(p,q,\omega)$ is obtained from the incident field at $z = 0$ by using

$$A(p,q,\omega) = \frac{\beta^2}{4\pi^2}\int\int \tilde{E}(x,y,0,\omega) \times \exp[-i\beta(px+qy)]\,dx\,dy. \tag{4}$$

We use the convention that integration limits, if unspecified, extend from $-\infty$ to ∞. The quantity m in Eq. (3) is defined as

$$m = \begin{cases} (1-p^2-q^2)^{1/2} & \text{if } p^2+q^2 \le 1, \\ i(p^2+q^2-1)^{1/2} & \text{otherwise.} \end{cases} \tag{5}$$

Eq. (3) is formally exact and can be used for numerical computations for an arbitrary pulsed optical beam. However, such an approach is time con-

suming numerically because of the triple integration and hinders physical insight. It is much more useful in practice to solve Eq. (3) approximately by making some reasonable assumptions. We make two simplifications. First, since the integration region $p^2+q^2>1$ corresponds to the contribution of evanescent waves, it can be ignored for distances $z \gg \lambda$, where $\lambda = 2\pi c/\omega$ is the wavelength. It should be stressed that the neglect of evanescent waves is justified here only because signal attenuation is taken to be negligible over the entire pulse spectrum assumed to be located far from medium resonances. If medium losses become significant, one must follow the recent analysis of Oughstun [13]. Second, we make the far-field approximation, valid when the propagation distance is much larger than the diffraction length (also called the Rayleigh range). By using Eqs. (4) and (5), the integrals over p and q in Eq. (3) can be evaluated analytically using the method of stationary phase [18], resulting in the following expression:

$$E(\mathbf{r},t) = \frac{\cos\theta}{ir}\int A\left(\frac{x}{r},\frac{y}{r},\omega\right)\frac{1}{\beta} \times \exp(i\beta r - i\omega t)\, d\omega. \tag{6}$$

where $r=(x^2+y^2+z^2)^{1/2}$ and θ is the diffraction angle ($\cos\theta = z/r$). Note that we have not made the paraxial approximation to allow for large diffraction angles. Eq. (6) is valid under quite general conditions and governs propagation of pulsed fields of arbitrary spatial and temporal profiles.

To make further analytical progress, we assume that the input beam incident at the plane $z=0$ has a Gaussian shape. The pulse shape is still arbitrary. More specifically, we use the following form for $\tilde{E}(x,y,0,\omega)$:

$$\tilde{E}(x,y,0,\omega) = \exp\left(-\frac{x^2+y^2}{2a^2(\omega)}\right)S(\omega), \tag{7}$$

where $a(\omega)$ is related to the spot size at $z=0$ and in general can depend on frequency. $S(\omega)$ is the complex spectral amplitude of the pulse and is normalized such that $\int S(\omega)\, d\omega = 1$. Using Eq. (7) in Eq. (4), we obtain

$$A(p,q,\omega) = \frac{\beta^2 a^2}{2\pi}\exp\left(-\frac{\beta^2 a^2}{2}(p^2+q^2)\right)S(\omega). \tag{8}$$

How does the beam waist a depends on the frequency ω? It is common to assume that a is a constant, independent of ω. This assumption holds if the input field can be factored as $E(x,y,0,t) = F(x,y)A_0(t)$, where $F(x,y)$ and $A_0(t)$ govern the beam shape and the pulse shape, respectively. However, there is some evidence in the literature on terahertz radiation that the beam waist a may change with the frequency ω such that the diffraction length, defined as $L_{\text{diff}} = \beta a^2$, is the same for all frequency components [12–16]. One may expect a similar behavior in other regions of the electromagnetic spectrum. Indeed, the beam waist in laser cavities also follows the same $\omega^{-1/2}$ dependence [19], making the diffraction length L_{diff} constant. For this reason, we consider both cases in this paper and refer to them as the ''constant beam waist'' and ''constant diffraction length'' cases.

The analysis so far applies for pulses of arbitrary duration. We now focus on the case in which the pulses are wide enough that they contain a few optical cycles at the carrier frequency ω_0. By using Eq. (8) in Eq. (6) and introducing the pulse envelope $A(\mathbf{r},t)$ through

$$E(\mathbf{r},t) = A(\mathbf{r},t)\exp\left[i(\beta_0 r - \omega_0 t)\right], \tag{9}$$

where β_0 is the value of β at the carrier frequency ω_0, we obtain the following expression for $A(\mathbf{r},t)$:

$$A(\mathbf{r},t) = \frac{\cos\theta}{2\pi ir}\int(\beta a^2)\exp\left[i(\beta-\beta_0)r - i \times(\omega-\omega_0)t - \tfrac{1}{2}\beta^2 a^2\sin^2\theta\right]S(\omega)\, d\omega. \tag{10}$$

The evaluation of the frequency integral in Eq. (10) requires knowledge of $\beta(\omega)$ as defined in Eq. (2). If the dispersion characteristics of the medium are known precisely through $n(\omega)$, one can use them to calculate the integral. This is the approach adopted for studying precursors when a pulse has a sharp leading or trailing edge [10]. It has also been used for diffraction of a delta-function pulse by using a Lorentz model for the dispersive medium [14]. The knowledge of the precise functional form of $n(\omega)$ is essential when the pulse spectrum is so wide that it overlaps with one (or more) atomic resonances of the medium. However, for pulses wider than a few optical cycles whose carrier frequency is far from

any medium resonances and whose shape is reactively smooth (no abrupt leading and trailing edges), the dispersive medium can be characterized by using the Taylor expansion of $\beta(\omega)$ around the carrier frequency ω_0 of the pulse [11]:

$$\beta(\omega) = \beta_0 + \beta_1(\omega - \omega_0) + \tfrac{1}{2}\beta_2(\omega - \omega_0)^2 + \cdots, \tag{11}$$

where $\beta_m = (d^m\beta/d\omega^m)_{\omega=\omega_0}$ with $m = 0,1,2,\cdots$. Here, β_1, β_2, etc. take into account dispersive effects at progressively higher orders. Physically, $\beta_1 \equiv 1/v_g$ is inversely related to the group velocity, and β_2 is called the GVD parameter since it takes into account the dispersion (frequency dependence) of the group velocity. The Taylor expansion (11) should be used with caution when it becomes necessary to include the third- and higher-order terms since the approximation becomes quite poor for long propagation distances and cannot be improved by just including more and more terms [20].

Using Eq. (11) and introducing a new dimensionless frequency variable $f = (\omega - \omega_0)T_0$, where T_0 is a measure of the input pulse width, Eq. (10) can be rewritten as

$$A(\boldsymbol{r},t) = \frac{\cos\theta}{2\pi i r}\int(\beta a^2) \times \exp\left(i\frac{\beta_2 r}{2T_0^2}f^2 - \tfrac{1}{2}\beta^2 a^2\sin^2\theta - if\tau\right) \times S(f)\,df, \tag{12}$$

where $\tau = (t - \beta_1 r)/T_0$ is the normalized ''reduced'' time. Eq. (12) requires a single integration that can be performed analytically in some special cases and provides considerable physical insight into the combined effects of dispersion and diffraction.

3. Nondispersive or weakly dispersive medium

We first consider the situation in which the medium is either nondispersive ($\beta_2 = 0$) or is weakly dispersive such that the propagation distance $r \ll L_{\text{disp}}$, where $L_{\text{disp}} = T_0^2/|\beta_2|$ is the so-called dispersion length [11]. In both cases, β_2 and higher-order dispersion parameters can be set to zero in the expansion (11). As discussed earlier, one may treat the beam waist a to be constant or frequency dependent such that the diffraction length is constant. We consider these two cases separately.

3.1. Constant beam waist

Assuming that the beam waist a does not depend on the frequency f in Eq. (12), we obtain

$$A(\boldsymbol{r},t) = F_{\text{cw}}(\boldsymbol{r})\int(1 + d_1 f) \times \exp\left(-\beta_0^2 a^2\sin^2\theta\, d_1 f - if\tau\right)S(f)\,df, \tag{13}$$

where

$$F_{\text{cw}}(\boldsymbol{r}) = \frac{\beta_0 a^2\cos\theta}{2\pi i r}\exp\left(-\tfrac{1}{2}\beta_0^2 a^2\sin^2\theta\right) \tag{14}$$

is the continuous-wave (CW) solution found when the input beam is not pulsed. The dimensionless parameter $d_1 = \beta_1/(\beta_0 T_0)$. The integral in Eq. (13) can be performed analytically for arbitrary pulse shapes and results in the following expression:

$$A(\boldsymbol{r},t) = F_{\text{cw}}(\boldsymbol{r})\left(1 + id_1\frac{d}{d\tau}\right)A_0(\tau - i\tau_s), \tag{15}$$

where $A_0(\tau)$ is the input pulse shape at the plane $z = 0$ and the parameter τ_s is defined as

$$\tau_s(\theta) = \beta_1\,\beta_0 a^2\sin^2\theta/T_0. \tag{16}$$

It is evident from Eq. (15) that the pulse characteristics are affected considerably even when dispersive effects are small or negligible. In general, the pulse shape is not preserved and is predicted to become asymmetric because of the presence of the time derivative in Eq. (15). However, the parameter d_1 is quite small since $d_1 \sim (\omega_0 T_0)^{-1}$, and the asymmetric nature of the pulse is not likely to be noticeable until pulse width is reduced below a few optical cycles. Since such pulses have now become available, for example from mode-locked Ti:sapphire lasers, one may be able to observe the asymmetry in actual experiments.

For pulses for which $\omega_0 T_0 \gg 1$, the pulse shape and the pulse spectrum are preserved only on axis ($\tau_s = 0$). Off axis ($\theta \neq 0$), Eq. (15) shows an imaginary shift of the pulse envelope. To understand the

meaning of such a shift, consider an unchirped Gaussian pulse for which $A_0(\tau) = \exp(-\tau^2/2)$. Since

$$A_0(\tau - i\tau_s) = \exp\left[-\left(\tau^2 - \tau_s^2\right)/2 + i\tau\tau_s\right], \qquad (17)$$

clearly the pulse peak is shifted and is located at $\tau = \tau_s$. At the same time, the pulse spectrum is shifted toward the red side. The temporal and spectral shifts both depend on the diffraction angle θ as indicated in Eq. (16) and vanish when $\theta = 0$. The origin of spectral shift is evident in Eq. (13), where the amplitude of each spectral component gets multiplied by a θ-dependent exponential factor. As a result, high-frequency components ($\omega > \omega_0$) are slightly damped, while the low-frequency components ($\omega < \omega_0$) are enhanced, shifting the spectrum toward the red side. Physically, low-frequency components diffract more than high-frequency components because of their smaller diffraction length, resulting in an apparent red shift in the pulse spectrum that increases as θ increases. As seen in Eq. (17), spectral changes also result in a shift in the intensity peak of the diffracted pulse.

3.2. Constant diffraction length

Assuming that the beam waist a depends on ω such that the diffraction length, $L_{\text{diff}} = \beta a^2$, is constant and using this fact in Eq. (12), we obtain the simple result

$$A(\boldsymbol{r},t) = F_{\text{cw}}(\boldsymbol{r})\, A_0(\tau - i\tau_s), \qquad (18)$$

where the θ-dependent parameter τ_s is now defined as

$$\tau_s(\theta) = \beta_1 L_{\text{diff}} \sin^2\theta/(2T_0). \qquad (19)$$

A comparison of Eqs. (15) and (18) shows two main differences in the case of constant diffraction length. First, the pulse shape does not change no matter how small the pulse becomes since the time-derivative term is absent. Second, the temporal and spectral shifts are reduced by a factor of two if we interpret $\beta_0 a^2$ in Eq. (16) as the average diffraction length.

The diffraction-induced temporal and spectral shifts can be substantial even at angles not too far from the axis of propagation. They can be observed in a nondispersive medium (or even free space). As an example, $\tau_s \sim 1$ for $\theta = 2^\circ$ if we use $T_0 = 50$ fs, $L_{\text{diff}} = 1$ cm, $v_g = 1/\beta_1 = 2 \times 10^8$ m/s and $\lambda_0 = 800$ nm, assuming a Ti:sapphire laser source. Even for such relatively wide pulses (full width at half maximum more than 80 fs), one can expect a spectral shift comparable to $1/T_0$, and a shift in the intensity-peak position comparable to T_0 when making measurements 2° off-axis. Such changes should be easily observable in practice. The pulse width remains unaffected since the effects of GVD have been neglected in this section.

4. Effects of group-velocity dispersion

When the effects of GVD are included by retaining the β_2 term in Eq. (11), the frequency integral in Eq. (12) cannot be performed in a closed form except for some specific input pulse shapes. We again consider the two cases of frequency-independent and frequency-dependent beam waists separately.

4.1. Constant beam waist

Assuming that the beam waist a does not depend on the frequency f in Eq. (12) and taking a Gaussian shape for the pulse spectrum (corresponding to a Gaussian-shaped input pulse), we obtain the following result:

$$A(\boldsymbol{r},t) = A_{\text{cw}}(\boldsymbol{r})\sqrt{\frac{1}{b}}\left(1 + id_1\frac{d}{d\tau} - \frac{d_2}{2}\frac{d^2}{d\tau^2}\right) \times \exp\left(-\frac{(\tau - i\tau_s)^2}{2b(z,\theta)}\right), \qquad (20)$$

where

$$b(z,\theta) = 1 + (\beta_0 a \sin\theta)^2\left(d_2 + d_1^2\right) - i\beta_0(z\sec\theta)\, d_2, \qquad (21)$$

and

$$d_1 = \frac{\beta_1}{\beta_0 T_0}, \quad d_2 = \frac{\beta_2}{\beta_0 T_0^2}. \qquad (22)$$

Eq. (20) shows how the combination of diffraction and dispersion affects a Gaussian pulse as it propagates in a linear dispersive medium. In general,

pulse shape does not remain Gaussian because of time derivatives appearing in Eq. (20). However, both d_1 and d_2 are quite small unless the pulse becomes so short that it lasts for only a few optical cycles. For Gaussian pulses for which $\omega_0 T_0 \gg 1$, one can neglect the time derivatives appearing in Eq. (20). Such Gaussian pulses remain approximately Gaussian on propagation although they experience temporal and spectral shifts, become chirped, and their width increases. The broadening factor B, defined as the increase in the pulse width relative to the input width, is found to be

$$B(z,\theta) = \left(\eta + \frac{z^2 \sec^2\theta}{\eta L_{\rm disp}^2}\right)^{1/2}, \tag{23}$$

where η is given by

$$\eta(\theta) = 1 + \mathrm{sgn}(\beta_2)\frac{L_{\rm diff}}{L_{\rm disp}}\sin^2\theta, \tag{24}$$

and the diffraction and dispersion lengths are defined as

$$L_{\rm diff} = \beta_0 a^2, \quad L_{\rm disp} = T_0^2/|\beta_2|. \tag{25}$$

We also assumed $d_2 + d_1^2 \approx d_2$ since $d_1^2/d_2 < 10^{-4}$ for most dispersive media.

The broadening factor B reduces to the well-known standard result [11], $B = [1 + (z/L_{\rm disp})^2]^{1/2}$, only for the on-axis case corresponding to $\theta = 0$. In the off-axis case, pulse width depends not only on θ but also on the relative magnitudes of the dispersion and diffraction lengths and the sign of β_2. Fig. 1 shows the broadening factor B as a function of θ for two values of the normalized propagation distance $Z = z/L_{\rm disp}$ in the cases of normal (dashed line) and anomalous (solid line) GVD assuming that the diffraction and dispersion lengths are equal. The diffracted Gaussian pulse is wider off axis in both cases but the broadening factor is quite different. Somewhat surprisingly, at a fixed far-field angle, pulse width is larger in the case of anomalous dispersion. In fact, the off-axis enhancement of the pulse width is barely noticeable in the normal-GVD case but can exceed a factor of two in the case of anomalous GVD. Although this prediction is made here using Gaussian pulses as an example, it holds qualitatively for other common pulses shapes.

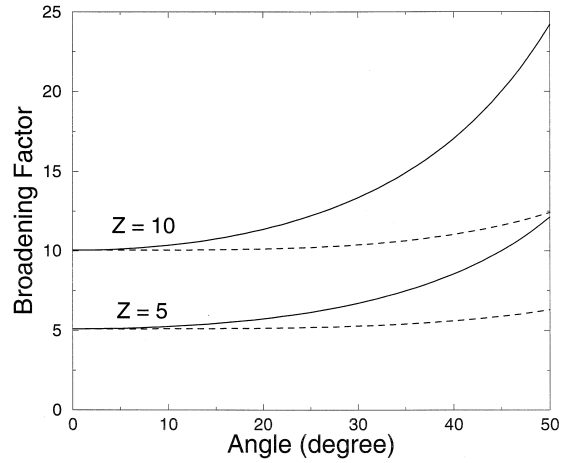

Fig. 1. Broadening factor B as a function of far-field angle θ for two values of $Z = z/L_{\rm disp}$ in the case of normal (dashed line) and anomalous (solid line) dispersion. The spot size of the input Gaussian pulse is assumed to be the same for all frequency components. The pulse and beam parameters are chosen such that the diffraction and dispersion lengths are equal.

4.2. Constant diffraction length

Assuming that the beam waist a depends on ω such that the diffraction length $L_{\rm diff} = \beta a^2$ is constant in Eq. (12) and using a Gaussian spectrum, we obtain the simple result

$$A(\boldsymbol{r},t) = A_{\rm cw}(\boldsymbol{r})\sqrt{\frac{1}{b}}\exp\left(-\frac{(\tau - i\tau_s)^2}{2b(z,\theta)}\right), \tag{26}$$

where $b(z,\theta)$ is now given by

$$b(z,\theta) = 1 + \beta_0 L_{\rm diff}\sin^2\theta d_2/2 - i\beta_0 z\sec\theta d_2. \tag{27}$$

A comparison of Eqs. (20) and (26) shows two main differences in the case of constant diffraction length. First, the pulse shape remains Gaussian no matter how small the pulse becomes since the time-derivative terms are absent. Second, the broadening factor is different because the second term in Eq. (27) is one half of that found for the case of constant width. In fact, the broadening factor is still given by Eq. (23) if η is redefined as

$$\eta(\theta) = 1 + \mathrm{sgn}(\beta_2)\frac{L_{\rm diff}}{2L_{\rm disp}}\sin^2\theta. \tag{28}$$

Fig. 2 shows the broadening factor B as a function of θ for two values of $Z = z/L_{\rm disp}$ in the normal (dashed line) and anomalous (solid line) GVD cases under conditions identical to those of Fig. 1 ($L_{\rm diff} = L_{\rm disp}$). A comparison of Fig. 1 and Fig. 2 shows a qualitatively similar behavior but substantial quantitative differences. More specifically, the enhancement in pulse width is lower in the case of constant diffraction length. Note also that in both cases, the off-axis enhancement factor is barely noticeable until the far-field diffraction angle exceeds 10°. This is the reason why the paraxial approximation was avoided in this paper. The results shown in Fig. 1 and Fig. 2 are valid for large diffraction angles as long as $z \gg L_{\rm diff}$.

4.3. Higher-order dispersive effects

As mentioned earlier, the Taylor expansion (11) should be used with caution when it becomes necessary to include the third- and higher-order terms. For pulses shorter than 1 ps but wide enough to contain several optical cycles, one may include the cubic term in the Taylor expansion provided certain conditions discussed in Ref. [20] are satisfied. In that case, it is no longer possible to carry out the frequency integral in Eq. (12) analytically, and one must resort to numerical simulations. However, Eq. (12) remains useful since it involves only a one-dimensional integration, in contrast with Eq. (12) involving a three-dimensional integration, that can be performed easily using the fast-Fourier-transform (FFT) algorithm. An additional advantage of the numerical approach is that optical pulses of arbitrary shape can be considered.

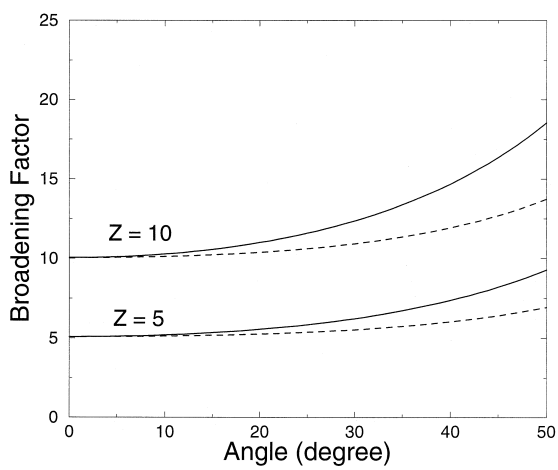

Fig. 2. Same as in Fig. 1 except that the spot size of the input Gaussian pulse depends on frequency such that the diffraction length is the same for all frequency components of the pulse. Solid and dashed lines correspond to the cases of anomalous and normal dispersion, respectively.

As an example, consider the propagation of ultrashort optical pulses through a silica glass slab. Dispersive properties of silica glass are well known (see, for example, Section 2.3 of Ref. [11]). In fact, the wavelength dependence of the refractive index for fused silica is well approximated by the the Sellmeier equation [21]

$$n^2(\lambda) = 1 + \sum_{j=1}^{3} \frac{B_j}{1 - \lambda_j^2/\lambda^2}, \tag{29}$$

where λ_j is a resonance wavelength and B_j is the corresponding oscillator strength. The parameters B_j and λ_j are determined empirically from experimental data and are found to be (for fused silica) $B_1 = 0.6961663$, $B_2 = 0.4079426$, $B_3 = 0.8974794$, $\lambda_1 = 0.0684043\ \mu$m, $\lambda_2 = 0.1162414\ \mu$m, and $\lambda_3 = 9.896161\ \mu$m. One can use this functional form in Eq. (10) and include dispersive effects to all orders for pulses of arbitrary shape. In practice, it is often sufficient to include dispersive effects only up to third order for pulses as short as 20 fs in the wavelength region near 1 μm. In that case, Eq. (12) can be written as

$$A(\boldsymbol{r},t) = \frac{L_{\rm diff}\cos\theta}{2\pi i r} \times \int \exp\left(\frac{i\beta_2 r_e f^2}{2T_0^2} + \frac{i\beta_3 r_e f^3}{6T_0^3} - i\tau f\right) \times S(f)\, df, \tag{30}$$

where $r_e = z\sec\theta + i\sin^2(\theta)L_{\rm diff}/2$. The frequency dependence of spot size was included assuming a constant diffraction length. This equation can be used for pulses of arbitrary shape. The main effect of third-order dispersion for both on- and off-axis measurements is to distort the pulse shape such that it becomes asymmetric and develops an oscillatory tail. Since these effects are well known [11], numerical results are not given here.

In Eq. (30), the parameters β_2 and β_3 vary with wavelength and have typical values $\beta_2 = -20$ ps^2/km and $\beta_3 = 0.1$ ps^3/km near 1.55 μm. Since the GVD is anomalous (negative β_2) for wavelengths larger than 1.27 μm, but normal otherwise, a silica glass slab is an ideal testing ground for verifying the prediction that off-axis pulse width depends on the nature of chromatic dispersion. One can use a Ti:sapphire laser capable of emitting femtosecond pulses at 780 nm, and the second-harmonic-generation technique can provide femtosecond pulses near 1.56 μm. As an example, both diffraction and dispersion lengths are about 1 cm for a pulsed optical beam with $T_0 = 50$ fs and $a(\omega_0) = 50$ μm. Propagation over a distance of 10 cm or show should show significant differences between the normal- and anomalous-dispersion regimes when pulse shapes and spectra are measured off axis.

5. Concluding remarks

This paper has considered propagation of a pulsed optical beam in a linear dispersive medium. The input beam is initially Gaussian (in transverse directions) but consists of a train of ultrashort optical pulses of arbitrary shape. The propagation problem is solved analytically by using the angular spectrum representation of electromagnetic fields. The analysis is simplified considerably making the far-field approximation but the paraxial approximation is avoided. This approach permits us to obtain analytical results that are valid for relatively large diffraction angles. Pulse characteristics are found to be affected considerably by the combination of diffraction and dispersion. They also depend on whether the spot size of the input beam is constant or depends on the frequency. We have considered both cases and compared the results.

In a weakly dispersive medium, pulses wider than a few optical cycles maintain their shape but experience temporal and spectral shifts whose magnitude depends on the diffraction angle. When the effects of group-velocity dispersion are included, the pulse width depends not only on the diffraction angle but also on the nature of GVD (normal versus anomalous). Much larger off-axis pulse widths are predicted for the case of anomalous GVD. We discuss the effects of third-order dispersion briefly and consider how a slab of silica glass can be used to verify the pulse-width dependence on the nature of GVD by using femtosecond pulses obtained from a Ti:sapphire laser.

Acknowledgements

The author thanks Dr. Hong Guo for a critical reading of the manuscript. The research is partially supported by the National Science Foundation, USA.

References

[1] I.N. Duling III (Ed.), Compact Sources of Ultrashort Pulses, Cambridge University Press, New York, 1995.
[2] I.P. Christov, in: E. Wolf (Ed.), Progress in Optics, vol. 29, Elsevier Science, Amsterdam, 1991, Chap. 3.
[3] A. Federico, O. Martinez, Opt. Commun. 91 (1992) 104.
[4] M. Kampe, U. Stamm, B. Wilhelm, W. Rudolph, J. Opt. Soc. Am. B 9 (1992) 1158.
[5] R.W. Ziolkowski, J.B. Judkins, J. Opt. Soc. Am. A 9 (1992) 2021.
[6] Z.L. Horváth, Z. Benko, A.P. Kovács, H.A. Hazim, Z. Bor, Opt. Eng. 32 (1993) 2491.
[7] Z. Wang, Z. Zhang, Z. Xu, Q. Lin, Opt. Commun. 123 (1996) 5; IEEE J. Quant. Electron. 33 (1997) 566.
[8] A.E. Kaplan, J. Opt. Soc. Am. B 15 (1998) 951.
[9] G.P. Agrawal, Opt. Commun. 157 (1998) 52.
[10] K.E. Oughstun, G.C. Sherman, Electromagnetic Pulse Propagation in Causal Dielectrics, Springer-Verlag, New York, 1994.
[11] G.P. Agrawal, Fiber-Opt. Commun. Systems, 2nd ed., Wiley, New York, 1997.
[12] T. Melamed, L.B. Felsen, J. Opt. Soc. Am. A 15 (1998) 1268; 1276.
[13] K.E. Oughstun, Pure Appl. Opt. 7 (1998) 1059.
[14] J.A. Solhaug, J.J. Stamnes, K.E. Oughstun, Pure Appl. Opt. 7 (1998) 1079.
[15] E. Budiarto, N.-W. Pu, S. Jeong, J. Bokor, Opt. Lett. 23 (1998) 213.
[16] S. Feng, H.G. Winful, R.W. Hellwarth, Opt. Lett. 23 (1998) 385.
[17] J. Bromage, S. Radic, G.P. Agrawal, C.R. Stroud Jr., P.M. Fauchet, R. Sobolewski, J. Opt. Soc. Am. B 15 (1998) 1953.
[18] L. Mandel, E. Wolf, Optical Coherence and Quantum Optics, Cambridge University Press, New York, 1995, Chap. 3.
[19] O. Svelto, Principles of Lasers, 4th ed., Plenum, New York, 1998, Chap. 5.
[20] K.E. Oughstun, H. Xiao, Phys. Rev. Lett. 78 (1997) 642.
[21] I.H. Malitson, J. Opt. Soc. Am. 55 (1965) 1205.